POST-COATING TREATMENT EFFECTS ON THE PHYSICOMECHANICAL AND CORROSION RESISTANCE OF PLASMA-SPRAYED HYDROXYAPATITE (FSHA) ON TI-13NB-13ZR ALLOY FOR BIOMEDICAL APPLICATIONS

Franklin Amaechi Anene[1,3], Che Nor Aiza Jaafar[1*], Ismail Zainol[2], Azmah Hanim Mohamed Ariff[1] and Suraya Mohd. Tahir[1]

[1]Department of Mechanical and Manufacturing Engineering, Faculty of Engineering, Universiti Putra Malaysia, Selangor, Malaysia.
[2] Department of Chemistry, Faculty of Science and Mathematics, Universiti Pendidikan Sultan Idris, Tanjong Malim, Perak, Malaysia.
[3] Department of Metallurgical and Materials Engineering, Faculty of Engineering, Nnamdi Azikiwe University, Awka, Nigeria.

*cnaiza@upm.edu.my

Abstract. β titanium alloys are widely used in orthopaedic applications as an alternative to the high modulus α + β titanium alloys which leads to aseptic loosening of implants as a result of the mismatch of the modulus to that of human bone. Hydroxyapatite (HA) coating has been used to enhance the biological properties of Ti alloys. The present study determined the effect of heat treatment on the properties of plasma-sprayed low modulus Ti-13Nb-13Zr alloy using a natural and economical HA derived from fish scales (FsHA) and FsHA-doped yttria stabilized zirconia (YSZ). The microstructure was examined by SEM-EDS and the hardness was determined using Vickers hardness tester whereas the corrosion resistance was studied using potentiodynamic polarization method. The SEM micrograph of the as-coated FsHA revealed micro pores and cracks with partially melted and unmelted FsHA particles while the as-coated FsHA/YSZ samples developed denser coatings, lesser number of pores with increased number of melted FsHA particles, fine micro cracks and evenly dispersed ZrO_2 particles. On the other hand, the post-coating treatment led to a much denser and finer lamellar morphology with more cracks as well as a significant increase in the microhardness as the heat-treated FsHA and FsHA/YSZ coatings had 514.7 and 566.9 Hv respectively, compared to their non-heat-treated values of 467.8 and 492.5 Hv. However, heat treatment recorded a slight increase in corrosion rate as the as-coated FsHA and FsHA/YSZ samples had 44.54 and 22.72 mmpy while their heat-treated counterparts recorded 83.7 and 73.88 mmpy respectively.

Key words: Hydroxyapatite coating, yttria stabilized zirconia, plasma spray, microhardness, corrosion resistance.

Article Info

Received 11th October 2021
Accepted 23rd November 2021
Published 20th December 2021

ISSN: 1823-7010, eISSN: 2600-7444

Introduction

Biomaterials have been exploited in tissue engineering, orthopaedic and dental applications as well as in drug delivery and cardiovascular devices due to their good biological properties [1]. Biomaterials are grouped into four main classes as: metals and their alloys, polymers, ceramics, and natural materials [2]. Metallic alloys like the Co-Cr alloys, 316L stainless steel, titanium-based alloys have dominated as the main biomaterials for implant productions such as in replacement implants in knees, shoulders, elbows, hips, and dental structures [3-4]. Among the metallic alloys used for orthopaedic implants, Ti and their alloys especially (CP)-Ti and Ti-6Al-4V (ELI) alloy are often used due to their good mechanical and biocompatibility properties [5]. Nevertheless, these implants have been reported to fail in vivo after long-term due to corrosion, fatigue, wear, and high modulus compared to the human bone [6]. Implants with higher modulus than the human cortical bone leads to unequal stress transfer to the bone resulting in implant loosening and failure in the long-term [6]. This is one of the disadvantages of α+β Ti alloys especially Ti-6Al-4V alloy with 110 GPa modulus compared to the 18-30 GPa modulus of human bone, in addition to its content of Al that has been associated with Alzheimer disease while V has potential toxicity [7-8]. To mitigate these demerits, low modulus (40-60 GPa) β-Ti alloys such as Ti-13Nb-13Zr, TMZF (Ti-Mo-Zr-Fe), Ti-15Mo, and TNTZ (Ti-Nb-Ta-Zr) alloys with other alloying elements other than Al and V, have been adopted.

Consequently, it is established that one of the ways of improving implants life is by coating their surfaces with a bioactive ceramic which promotes early bonding of bone tissues with the implant surface as well as the adhesion of hydroxyapatite (HA) [9]. Plasma spraying is the commercially adopted coating technique for HA due to its advantages of simplicity with high rates of uniform powder deposition as well as moderate substrate temperature. Plasma coating involves production of an ionized gas (plasma) in which HA powder is injected, partially melted, and projected to splat on a substrate at a controlled distance from the spraying gun [10-11]. Bone is made up of organic and inorganic components that gives it flexibility, strength, and toughness. The organic components are the collagen, glycoproteins, fibrillin, and proteoglycans while the inorganic component is HA [12]. HA is a mineral form of calcium apatite found use as bone grafting material and dental prosthetics. It can be naturally fabricated from coral, bovine bone, fish bone, fish scales, and eggshells [13]. HA has been the dominant coating material for implants, although, other bioactive materials such as calcium phosphate (CaP), tricalcium phosphate ($Ca_4(PO_4)_2O$) TCP and β-tricalcium phosphate (β-TCP), fluoridated HA (FHA), carbonated HA (CHA), oxyhydroxyapatite (OHA), Oxyapatite (OA) [13] are also in use.

HA possesses excellent biocompatibility and osteoconductivity with human body fluid which favours early bonding between bone tissues and the implant surface [14-15], however, their low mechanical properties like brittleness, tensile strength, fretting fatigue, adhesive strength, toughness, and poor impact resistance have limited their use in some load bearing applications [16]. Hence, the reinforcement of HA with bioinert ceramics or metal powders or fibres have been used to enhance their mechanical properties. Fu et al., [17], reported improved mechanical properties with plasma-sprayed HA/ZrO_2 coating compared to the HA alone while enhanced corrosion resistance was reported by Singh et al., [18] with plasma-sprayed HA/SiO_2 composite coating on AlSi 304 alloy. Despite the merits of HA coating on Ti alloy implants, some drawbacks have also been reported such as the formation of cracks at the coating interface layers induced by thermal stresses as a result of the difference in the thermal expansion between the HA ceramic and Ti alloys. These cracks can

result in a compromised adhesion strength of the coating. Similarly, chemical reactions between the ceramic and the substrate at the interface can adversely affect the coating strength [9]. Heat treatment can be the procedure to mitigate these demerits and enhance the mechanical properties of FsHA/YSZ bioceramic coating on low modulus Ti-13Nb-13Zr alloy.

Thus, in this research the effect of HA and YSZ modified HA coating on Ti-13Nb-13Zr alloy was examined on the microstructure, microhardness, and corrosion rate. Also, the use of natural and economical HA derived from fish scales will aid waste management, checkmate environmental pollution, and reduce the cost of implants. Similarly, natural HAs contain trace elements like Na, Mg, Si, Zn, and K which mimics the apatite formed by human bone that is vital in bone regeneration and accelerating bone formation process [19].

Materials and methods

Powder preparation. Spray drying technique was used to produce the FsHA powders used in this research from fish scale slurry previously produced by the authors [20]. The FsHA powders were then calcined at 1200 ℃ for 2 h to increase their crystallinity, mechanically sieved thereafter and powders with 50 -150 µm particle sizes collected. Subsequently, the FsHA powders and fine powders of yttria stabilized zirconia -YSZ (ZrO_2-8wt% Y_2O_3) at 10 wt% compositions were mechanically mixed, ball milled with a planetary ball mill having a cylindrical alumina bowl and alumina balls operated at a rotatory speed of 100 rpm for 15 h, then oven dried at 100 ℃ and sieved. The resulting powders in the range of 60 – 100 µm were used as feedstock for the plasma coating.

Plasma coating and heat treatment. Ti-13Nb-13Zr alloys with $25 \times 10 \times 4\ mm$ dimensions served as the substrate. The samples were ground using silicon carbide papers (180-1200) grits respectively in a grinding machine, ultrasonically washed for 30 min with acetone, ethanol, and deionized water. The samples were subsequently grit blasted with alumina of 50-60 µm particle sizes at 5 bars pressure for 3 min and finally air blasted for removal of any residual grit. The powder depositions after grit blasting were done using the Quarom-platinum target plasma coating machine. Argon gas was used as the primary plasma forming gas and carrier gas while helium gas was the secondary gas. The substrates were kept at standoff distance of 100 mm and current of 500 A used for the spraying at 250 mm/s gun transverse speed with powder feed rate of 15 g/m. After the plasma coating, post coating heat treatment was done at 750 ℃ for 1h at a heating rate of 5 ℃/m in a nitrogen gas furnace and subsequently furnace cooled.

Microstructure analysis. The coated and heat-treated samples were ground with 320 and 1000 grits silicon carbide papers using 6 µm monocrystalline diamond suspension and polished with 0.05µm MasterPrep polishing suspension. The polished samples were finally etched for 20 sec in Kroll's reagent and stored in a desiccator for further analysis. Scanning electron microscopy (SEM) (Model: Leo 1455 VP) equipped with energy dispersive spectroscopy (EDS) was used to examine the microstructure of the coatings and identify the elements within the coatings.

Microhardness test. Microhardness test of the bioceramic coatings and the uncoated substrate were determined using Wolpert group digital micro-Vickers hardness tester with

300 gf load and 10 sec dwell time. The indentations were made from the top of the coatings through the substrate adhering to ASTM E92 standards. After the indentation, the D_1 and D_2 diagonal measurements of the diamond pyramid were measured, and the hardness values automatically given by the equipment recorded. Each test was repeated thrice at different positions of at least 1mm gap and the average values recorded.

Electrochemical corrosion test. Potentiodynamic polarization tests were carried out to study the electrochemical corrosion behaviour of the uncoated and plasma coated samples. Potentiostat/Galvanostat/ZRA (Gamry instrument Ref 3000) having Gamry electrochemical software DC 105 was used for the test. Phosphate buffered saline (PBS) which is a water-based salt solution containing 8 g NaCl, 0.2 g KH_2PO_4, 2.9 g $Na_2HPO_4.12H_2O$ and 0.2 g KCl in 100 ml of solution at a pH 7.4 was used as the electrolyte for simulating human body fluid conditions. Prior to the corrosion test, the samples were immersed in the electrolyte for 3 h at 37 ℃ for stabilization and the exposed area of the samples to the electrolyte during the corrosion test was 1 cm^2. The coated Ti-13Nb-13Zr alloy was used as the working electrode, standard Ag/AgCl was used as the reference electrode while graphite rod served as the counter electrode. The Gamry framework measures and controls the potential difference between the reference electrode and the working electrode. The tests were conducted at 1mV/sec scan rate for 1h to establish a steady-state open circuit potential (OCV) and fresh electrolyte was used for each test while the polarization curves were initiated at $-250\ mV\ to + 250\ mV$ relative to the open circuit potential. The equivalent weight of Ti-13-13Zr alloy used was 13.42 as calculated from equation (1) and Table 1. [21].

$$\text{Equivalent weight (EW)} = \frac{1}{\sum \frac{\text{NiFi}}{\text{Mi}}} \quad (1)$$

where Ni = valency of the element in the alloy, Fi = mass fraction of the elements in the alloy, and Mi = atomic weight of the elements in the alloy.

Table 1. Calculation of equivalent weight of Ti-13Nb-13Zr alloy.

Ti-13Nb-13Zr				
Element	**Fi**	**Ni**	**Mi (g/mol)**	**NiFi/Mi**
Ti	0.74	4	47.90	0.0618
Nb	0.13	5	92.91	0.007
Zr	0.13	4	91.224	0.0057

Also, the corrosion rate is calculated using equation (2)

$$CR = 0.13 \times \frac{Icorr \times Ew}{\rho} \quad (2)$$

where, Icorr is the corrosion current density, Ew is the equivalent weight and ρ is the density.

Results and Discussion

Microstructure analysis. The SEM micrographs of plasma sprayed FsHA and FsHA + 10 wt% YSZ coatings and their respective heat-treated micrographs are shown in Figure 1, while Fig 2 represents the different spectrums analysed by EDS and their respective elemental graphs. It is observed that the surface morphology of the as-coated FsHA sample (Figure 1a) contains unmelted spheroidized FsHA particles, molten solidified FsHA particles

that formed a dense coat and the presence of micro cracks. Similarly, the micrograph of the heat-treated FsHA coating (Figure 1c) revealed a much denser and finer lamellar morphology with cracks, unmelted and partially melted FsHA particles. The EDS analysis at four different spectrums on the micrograph confirmed the strong presence of FsHA by the significant amounts of Ca^{2+} and P^{3-} ions present (Figure 2a). Figure 1 (b & d) represents the SEM micrographs of as-coated and heat-treated FsHA + 10wt% YSZ samples which shows partially melted and unmelted FsHA particles, white chunk of ZrO_2 particles and small inter-lamellar evenly dispersed white dots of molten solidified ZrO_2 particles. The addition of YSZ led to the arrest of cracks witnessed with the undoped coating while heat treatment developed finer morphology, denser coating with micro cracks. The EDS analysis on four spectrums of the coating (Figure 2b) indicates good presence of Ca^{2+} and P^{3-} ions as well as a significant amount of ZrO_2 particles representing the white chunk region.

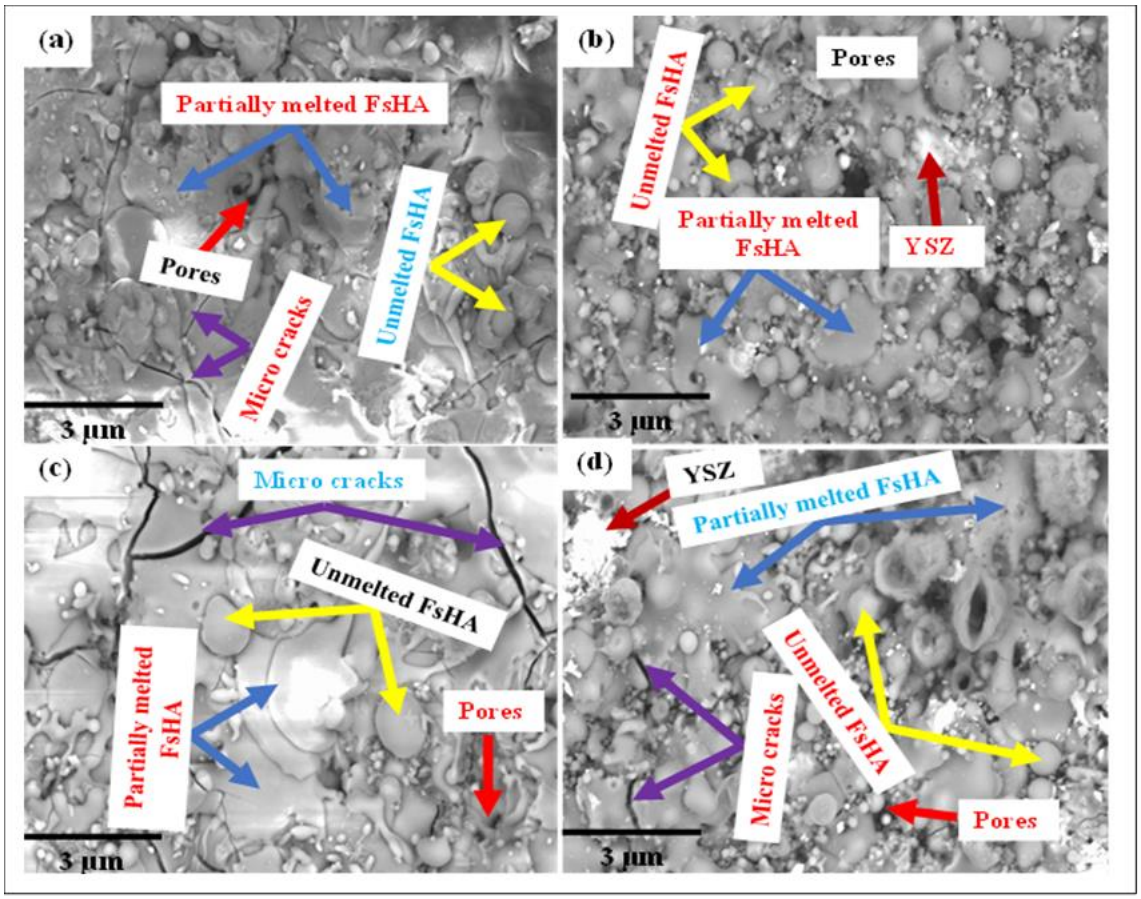

Figure 1. SEM micrographs (1kX) of plasma coated Ti-13Nb-13Zr alloy substrates (a) FsHA, (b) FsHA + 10wt% YSZ, (c) Heat-treated FsHA, and (d) Heat-treated FsHA + 10wt% YSZ Plasma coatings.

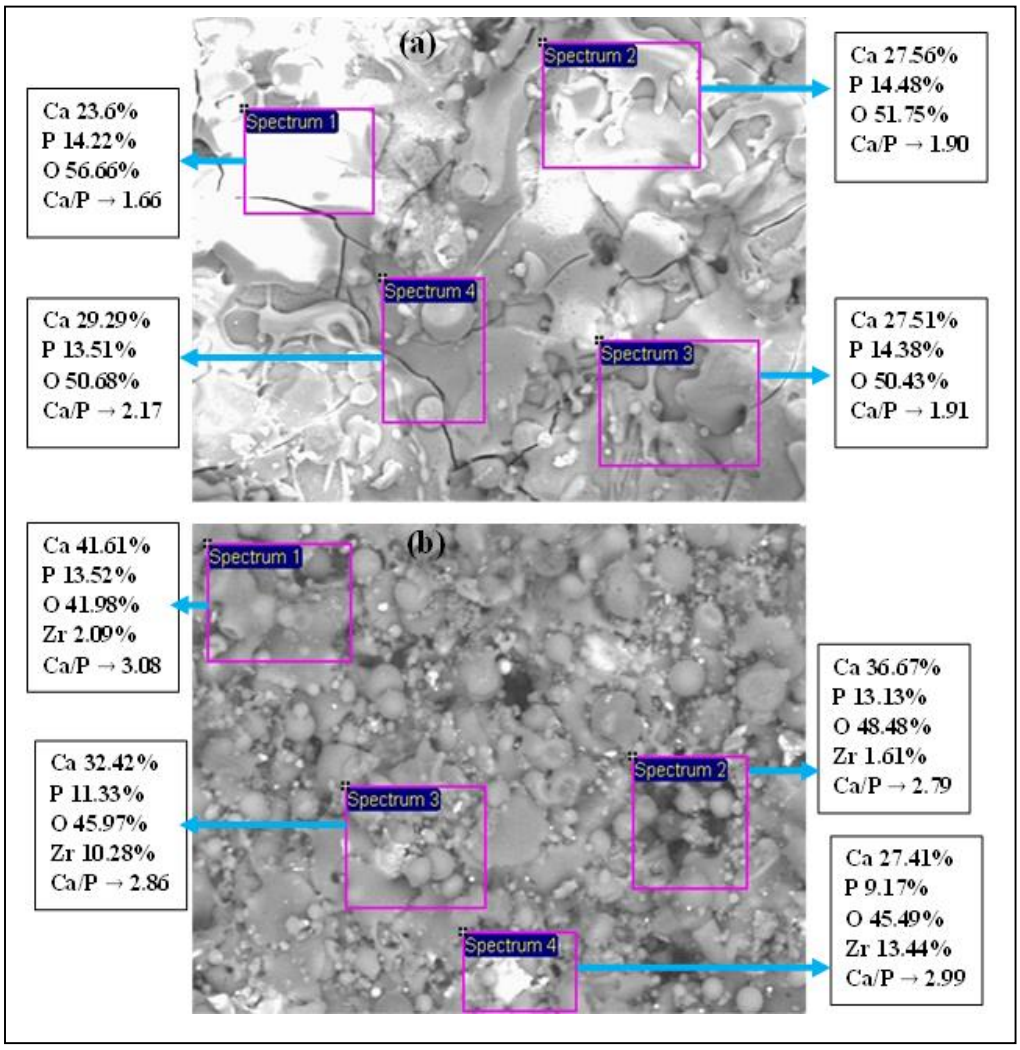

Figure 2. EDS elemental analysis (a) FsHA coating and (b) FsHA + 10wt% YSZ coating.

Microhardness. Microhardness of coatings measures the resistance of a coating to plastic deformation. Shown in Figure 3 and Table 2 is the hardness values of the uncoated substrate, as-coated and heat-treated FsHA and FsHA + 10 wt% YSZ coatings. The result shows that heat treatment had a significant improvement in hardness compared to the non-heat-treated samples and uncoated substrate. The heat-treated FsHA and FsHA + 10 wt% YSZ coatings recorded 10 % and 15 % increments in hardness compared to their non-heat-treated samples while heat-treated FsHA + 10 wt% YSZ sample with the maximum hardness had a 47 % increment in hardness compared to the uncoated substrate. This improvement in hardness with heat treatment indicates a high resistance of the coating to plastic deformation. Also, YSZ doping to FsHA introduced evenly dispersed ZrO_2 particles within the matrix leading to dispersion strengthening mechanism and in line with other reported works [17].

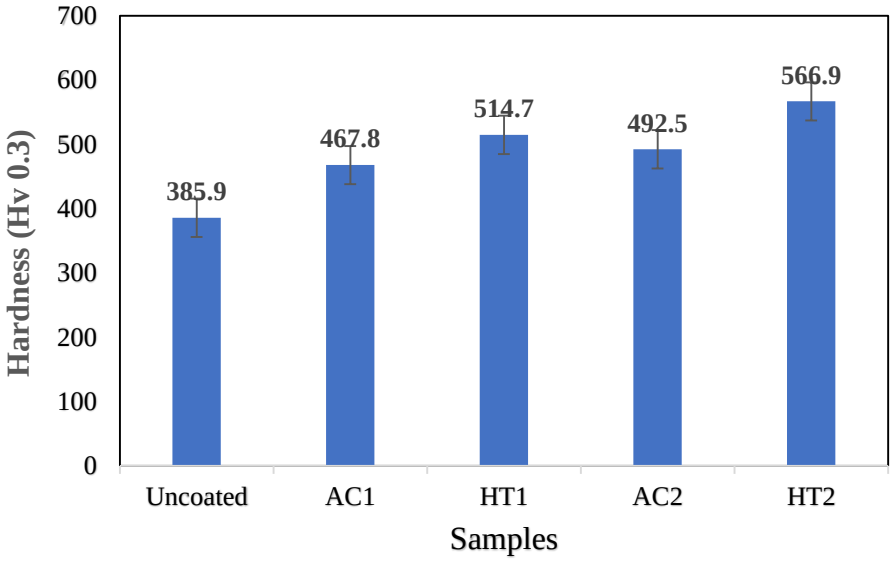

Figure 3. Microhardness chart where AC1 and AC2 represent the as-coated FsHA and FsHA + 10wt% YSZ coatings while HT1 and HT2 represent their corresponding heat treatments.

Table 2. Result of the potentiodynamic and microhardness tests.

Parameters	Uncoated	AC-FsHA	HT-FsHA	AC-FsHA + 10wt% YSZ	HT-FsHA + 10wt% YSZ
βa (mV/decade)	291.4	276.2	281.7	263	256.6
βc (mV/decade)	147.9	135.6	139.5	92.77	122.0
Ecorr (mV)	-563	-409.6	-209.6	-245	-296
Icorr (nA)	370	128.7	242	65.67	213.5
CR (mmpy)	128.1	44.54	83.7	22.72	73.88
OCV (mV)	-552.7	-331	-111.6	-176	-195.7
Hardness (Hv 0.3)	385.9	467.8	514.7	492.5	566.9

Corrosion behaviour. The ability of metallic alloy implants coated with ceramics to last long in vivo with high corrosion resistance is a prerequisite in clinical use. The potentiodynamic scans of the uncoated substrate and the heat-treated FsHA and FsHA/YSZ coatings in PBS solution are shown in Figure 4. The following corrosion parameters were evaluated using the Tafel extrapolation method from the potentiodynamic curves: anodic Tafel slope (βa), cathodic Tafel slope (βc), corrosion potential (Ecorr), corrosion current density (Icorr), and corrosion rate (CR). Table 2 presents the corrosion results with slight reduction in corrosion resistance observed in heat-treated samples compared to the non-heat-treated samples. This could be linked to the development and expansion of micro cracks as seen from their SEM micrographs, however, they recorded improved corrosion rate compared to the uncoated substrate. The heat-treated FsHA and FsHA + 10 wt% YSZ coatings recorded 35 % and 42 % improvement in corrosion resistance to the uncoated substrate which is in

agreement with related published works [18]. Also, the corrosion current density (Icorr) of all the heat-treated samples had lesser Icorr values than the uncoated substrate indicating improved corrosion resistance as corrosion rate of a material at a given potential is proportional to the corrosion current density.

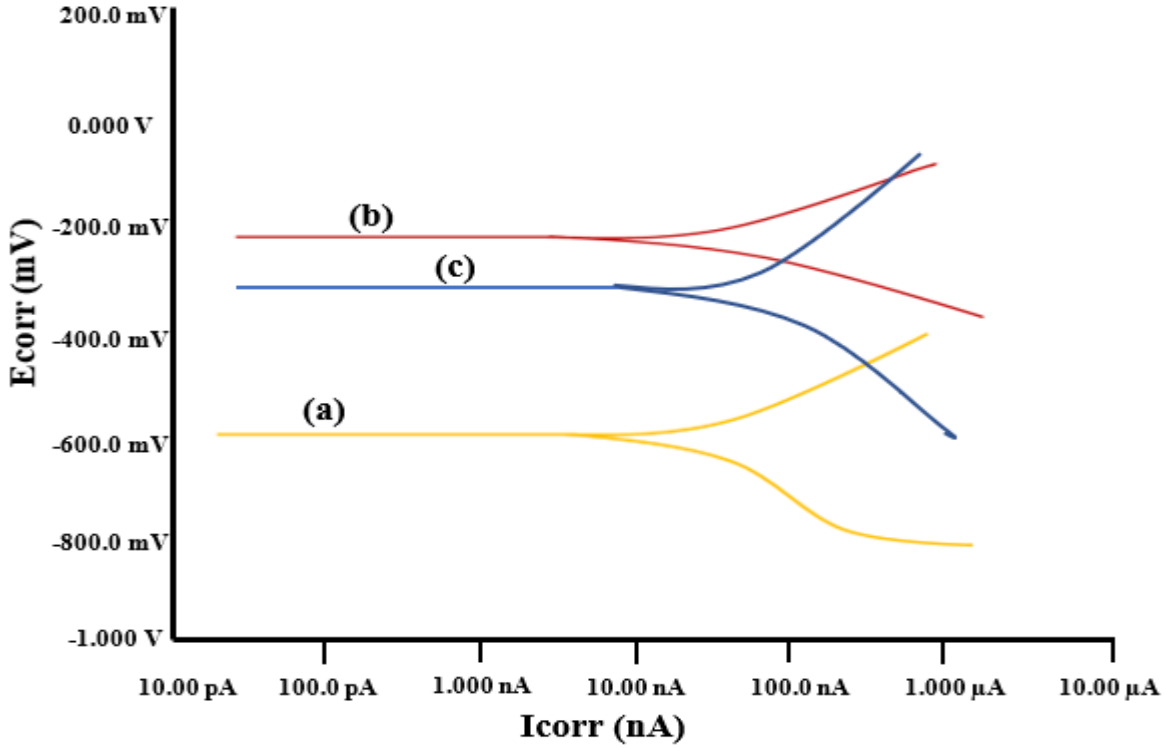

Figure 4. Potentiodynamic scans of (a) uncoated Ti-13Nb-13Zr alloy substrate, (b) heat-treated FsHA, and (c) heat -treated FsHA + 10wt% YSZ Plasma coatings.

Conclusion

The following conclusions were drawn from this study that investigated the microstructure, microhardness, and corrosion behaviour of heat-treated plasma sprayed FsHA and FsHA + 10 wt% YSZ coatings on Ti-13Nb-13Zr alloy substrate.

1. The SEM micrograph of heat-treated FsHA coating revealed micro-cracks, partially melted and unmelted FsHA particles while the heat-treated FsHA + 10 wt% YSZ coating developed minor cracks with partially melted and unmelted spheroidized FsHA particles in addition to evenly dispersed ZrO_2 particles within the matrix. Also, the EDS analysis showed strong presence of Ca^{2+} and P^{3-} ions and adequate Ca/P ratios.
2. The heat-treated FsHA + 10 wt% YSZ sample recorded the best hardness (566.9 Hv) compared to the undoped (467.8 Hv) and uncoated substrate (385.9 Hv). This is linked to the solid-solution dispersion strengthening mechanism of YSZ in FsHA coated matrix.
3. Heat-treated FsHA and FsHA/YSZ coatings with corrosion rates of 83.7 and 73.88 mmpy respectively, shows a slight reduction in corrosion resistance in relation to their non-heat-treated counterparts of 44.54 and 22.72 mmpy corrosion rates respectively.

However, they presented superior corrosion resistance compared to the uncoated substrate with 128.1 mmpy corrosion rate.

4. Heat treatment of FsHA coatings is therefore recommended based on our findings, however, other heat treatment temperatures (500, 600, 650, and 700 ℃) and times (30, 45, 60, 90, and 120 mins) should also be investigated.

Acknowledgements

The authors gratefully acknowledge Universiti Putra Malaysia for the financial support provided through the Putra Grant-IPS (GP-IPS/2020/9683900) and the Strength of Materials Laboratory, Mechanical and Manufacturing Engineering Dept, UPM where the research was conducted as well as the Chemistry Department, UPSI, Malaysia for some of the test analyses.

Author Contributions

All authors contributed toward data analysis, drafting and critically revising the paper and agree to be accountable for all aspects of the work.

Disclosure of Conflict of Interest

The authors declare no potential conflict of interest in the publication of this work.

Compliance with Ethical Standards

The work is compliant with ethical standards.

References

[1] Park, J. B. & Bronzino, J. D. (2003). *Biomaterials: principles and applications*, CRC Press, Boca Rator.

[2] Langer, R. & Peppas, N. A. (2003). Advances in biomaterials, drug delivery, and bionanotechnology, *AIChE J.* (49) 2990-3006.

[3] Aherwar, A., Singh, A. K. & Patnaik, A. (2016). Cobalt Based Alloy: A Better Choice Biomaterial for Hip Implants. *Trends Biomater. Artif. Organs.*, 30(1) 50-55.

[4] El-Zayat, B. F., Ruchholtz, S., Efe, T., Paletta, J., Kreslo, D. & Zettl, R. (2013). Results of titanium locking plate and stainless-steel cerclage wire combination in femoral fractures. *Indian J. Orthop.*, 47(5) 454–458.

[5] Singh, R. & Dahotre, N. B. (2007). Corrosion degradation and prevention by surface modification of biometallic materials. *J. Mater. Sci. Mater. Med.*, 18, 725–751.

[6] Geetha, M., Singh, A. K., Asokamani, R. & Gogia, A. K. (2009). Ti-based biomaterials, the ultimate choice for orthopaedic implants – A review. *Prog. Mater. Sci.* 54, 397–425.

[7] Rao, S., Ushida, T. & Tateishi, T. (1996). Effect of Ti, Al, and V ions on the relative growth rate of fibroblasts (l929) and osteoblasts (mc3t3-e1) cells. *Bio-Med Mater Eng.* (6) 79-86.

[8] Zaffe, D., Bertoldi, C. & Consolo, U. (2004). Accumulation of aluminium in lamellar bone after implantation of titanium plates, Ti-6Al-4V screws, hydroxyapatite granules. *Biomaterials*, 25 3837.

[9] Renganathan, G., Tanneru, N. & Madurai, S. L. (2018). Orthopaedical and biomedical applications of titanium and zirconium metals. In: *Fundamental biomaterials: metals*. (Sawston: Woodhead Publishing) 211–241.

[10] Yang, Y., Kim, K. H., Ong, J. L. (2005). A review on calcium phosphate coatings produced using a sputtering process: an alternative to plasma spraying. *Biomaterials*, (26) 327–337.

[11] Fernandez, J., Gaona, M. & Guilemany, J. M. (2004). Tribological study of plasma hydroxyapatite coatings. *Key Eng. Mat.* 16 383–386.

[12] Ghosh, S., Sanghavi, S. & Sancheti, P. (2018). Metallic biomaterial for bone support and replacement. In: *Fundamental Biomater: Metals*. (Woodhead Publishing) pp. 139-165

[13] Surmenev, R. A., Surmeneva, M. A. & Ivanova, A. A. (2014). Significance of calcium phosphate coatings for the enhancement of new bone osteogenesis: a review. *Acta Biomater*, (10) 557–579.

[14] Suchanek, W. & Yoshimura, M. (1998). Properties of hydroxyapatite-based biomaterials for use as hard tissue replacement implants. *J. Mater. Res.*, (13) 94 -117.

[15] De Bruijn, J. D., Van Blitterswilk, C. A. & Davis, J. E. (1995). Initial bone matrix formation at the hydroxyapatite interface in vivo. *J. Biomed. Mater. Res.*, (29) 89–99.

[16] Grootde, K., Wolke, J. G. C. & Jansen, J. A. (1998). Calcium phosphate coatings or medical implants. *Proc. Inst. Mech. Eng.*, H 212, 137–147.

[17] Fu, L., Khor, K. A. & Lim, J. P. (2002). Effects of yttria stabilized zirconia on plasma sprayed hydroxyapatite/yttria stabilized zirconia composite coatings. *J Am Ceram Soc*., (85) 800–806.

[18] Singh, G., Singh, H. & Sidhu, B. S. (2013). Corrosion behaviour of plasma sprayed hydroxyapatite and hydroxyapatite-silicon oxide coatings on AISI 304 for biomedical application. *Applied Surface Science*, (284) 811– 818.

[19] Akram, M., Ahmed, R., Shakir, I., Ibrahim, W. A. W. & Hussain, R. (2014). Extracting hydroxyapatite and its precursors from natural resources. *J. Mater. Sci*., (49) 1461–1475.

[20] Zainol, I., Adenan, N. H. & Rahim, N. A. (2019). Extraction of natural hydroxyapatite from tilapia fish scales using alkaline treatment. *Materials Today: Proceedings.,* (16) 1942–1948.

[21] Burnat, B., Walkowiak-Przybyło, M., Błaszczyk, T. & Klimek, L. (2013). Corrosion behaviour of polished and sandblasted titanium alloys in PBS solution. *Acta of Bioengineering and Biomechanics*, (15) 1-9.